



## Regular article

# Complex of hydrogel with magnetic immobilized GOD for temperature controlling fiber optic glucose sensor



Jun Huang<sup>a,b,\*</sup>, Peipei Zhang<sup>a,b</sup>, Mengshi Li<sup>a,b</sup>, Pengfei Zhang<sup>a,b</sup>, Liyun Ding<sup>a,b</sup>

<sup>a</sup> State Engineering Laboratory for Fiber Optic Sensing Technology, Wuhan University of Technology, Wuhan, 430070, China

<sup>b</sup> Key Laboratory of Fiber Optic Sensing Technology and Information Processing, Wuhan University of Technology, Ministry of Education, Wuhan, 430070, China

## ARTICLE INFO

## Article history:

Received 12 May 2016

Received in revised form 4 July 2016

Accepted 20 July 2016

Available online 21 July 2016

## Keywords:

P(NIPAAm-co-AAm)

PMIGC

Temperature controlling

Fiber optic glucose sensor

## ABSTRACT

A fiber optic glucose biosensor based on Poly(N-isopropylacrylamide-co-acrylamide) (P(NIPAAm-co-AAm))-magnetic-immobilized glucose oxidase (GOD) complex (PMIGC) was fabricated to perform the controllable detection of glucose by changing temperature. The complex was prepared by combining P(NIPAAm-co-AAm) with GOD immobilized on  $\text{Fe}_3\text{O}_4@\text{SiO}_2(\text{F})@\text{meso-SiO}_2$  nanoparticles using in-situ complex method. Since P(NIPAAm-co-AAm) has the lower critical solution temperature (LCST) of  $36^\circ\text{C}$ , at the temperature above LCST, P(NIPAAm-co-AAm) shrank and PMIGC could not catalyze the oxidation of glucose. At the temperature below LCST, P(NIPAAm-co-AAm) swelled and catalysis occurred. Because of this temperature sensing characteristics of PMIGC, the temperature controllable detection of glucose can be carried out by the biosensor. The optimal detection conditions for this biosensor were achieved with pH 6.5,  $35^\circ\text{C}$  and 12 mg of GOD amount. At  $25^\circ\text{C}$ , a good linear relationship between  $\phi$ , the phase delay change of the sensor head, and the glucose concentration in the range of 50–700 mg/dL (2.78–38.89 mmol/L) was observed, the detection limit was 8.33 mg/dL (0.46 mmol/L) (S/N = 3). This linear graph can be defined by the equation of  $y = 0.01463 + 0.0003313x$ ,  $R^2 = 0.9914$ . The biosensor has the characteristics of good repeatability and selectivity, and can be used for the glucose detection in practical samples.

© 2016 Elsevier B.V. All rights reserved.

## 1. Introduction

Glucose is very important for the life cycles but the high level of glucose in blood could cause diabetes. In recent years, more and more people around the world are suffering from the long-term risks of diabetes complications, such as heart disease, cardiovascular diseases and blindness [1,2]. Therefore, it is very urgent to develop a fast, reliable and economic method for the determination of blood glucose concentration.

Over the last few decades, many methods have been developed to detect glucose, including high performance liquid chromatography (HPLC) [3,4], colorimetry [5], spectrophotometry [6], chemiluminescence [7,8], electrode [9–11], electrochemical sensor [12,13], quantum dots sensing [14–16] and optical sensing [17–19]. Fiber optic biosensors have many advantages compared with electrical sensors and electrochemical sensors [20]. As a branch of fiber

optic sensors, the enzyme based fiber optic biosensors have great application potential in many fields and will be an effective way to detect glucose. If the enzyme performance can be controlled, the detection of glucose by the enzyme based fiber optic biosensors can be controlled, which will have important applications in many cases.

Stimuli-sensitive hydrogels have tunable three-dimensional physical network structures and good biocompatibility [21]. Their volumes will change with a slight variation of external stimuli, such as temperature, light, chemical environment, etc [22]. Thermo-sensitive hydrogels have a lower critical solution temperature (LCST), and will swell at the temperature lower than LCST and shrink at the temperature higher than LCST. Because of this characteristic, hydrogels have been extensively used as the carriers for the temperature controlled release of macromolecular drugs [23–25]. Poly(N-isopropylacrylamide) (PNIPAAm) is a well known temperature sensitive polymer with a LCST of  $\sim 32^\circ\text{C}$  in aqueous solution [26]. The introduction of segment acrylamide (AAm) to the PNIPAAm could form Poly(N-isopropylacrylamide-co-acrylamide) (P(NIPAAm-co-AAm)), which could slightly increase its LCST [23] and made the LCST close to human body temperature. If P(NIPAAm-

\* Corresponding author at: State Engineering Laboratory for Fiber Optic Sensing Technology, Wuhan University of Technology, Wuhan, 430070, China.  
E-mail address: [hjun@whut.edu.cn](mailto:hjun@whut.edu.cn) (J. Huang).

co-AAm) is used to form a complex with enzyme, the hydrogel will shrink at the temperature higher than its LCST and the enzyme is isolated from the substrate, which will cause the enzymatic catalysis reaction to stop. On the other hand, when the temperature is lower than its LCST, the hydrogel will swell, which allows the enzyme to have contact with the substrate and cause the enzymatic catalysis reaction to take place. Therefore, the enzyme performance can be controlled by changing the temperature. This kind of complex materials can be used for the fiber optic biosensor to perform controllable detection, and also for multi parameters fiber optic biosensors which can detect different species such as glucose and cholesterol at different temperature.

In our previous work [27], the magnetic fluorescent core-shell structured  $\text{Fe}_3\text{O}_4@/\text{SiO}_2(\text{F})@/\text{meso-SiO}_2$  nanoparticles were prepared. Cholesterol oxidase (COD) was immobilized on their surface and immobilization conditions were investigated and optimized. In this work, Glucose oxidase (GOD) was immobilized on  $\text{Fe}_3\text{O}_4@/\text{SiO}_2(\text{F})@/\text{meso-SiO}_2$  nanoparticles using the similar method [27]. P(NIPAAm-co-AAm) was combined with magnetic immobilized GOD to form P(NIPAAm-co-AAm)-magnetic immobilized GOD complex (PMIGC) using in-situ complex method. The immobilization of GOD will improve the enzyme stability and the nanoparticles with the magnetic core will be beneficial to the isolation of the immobilized enzyme from the reaction mixture. By changing temperature, the oxidation of glucose was controlled using PMIGC as the catalyzer. Using lock-in technology, a fiber optic glucose sensor based on PMIGC was fabricated to perform the controllable detection of glucose and the sensor properties were studied. The sensor can detect glucose effectively, indicating a promising prospect of practical application. To the best of our knowledge, there have been no publications on this temperature controlling fiber optic glucose biosensor based on PMIGC.

## 2. Experimental

### 2.1. Materials

Glucose oxidase (GOD) (E.C. 1.1.3.4, 100 U  $\text{mg}^{-1}$ ) was obtained from Aspergillusniger. Glucose,  $\text{Ru}(\text{bpy})_3\text{Cl}_2$  (99.0%) were purchased from Aldrich-Sigma. N-isopropylacrylamide (NIPAAm) was purchased from Aldrich Chemical Co. Inc. (USA), and was recrystallized from benzene/n-hexane. Acrylamide (AAm), Ammonium persulfate (APS), N,N'-Methylenebisacrylamide (BIS), N,N,N',N'-Tetramethylethylenediamine (TEMED) were purchased from Sinopharm Chemical Reagent Co. All reagents were of analytical grade and used without further purification. Double-distilled water was used throughout the experiments. The oxygen sensing membrane was prepared according to our previously work [28].

### 2.2. Preparation of PMIGC

$\text{Fe}_3\text{O}_4@/\text{SiO}_2(\text{F})@/\text{meso-SiO}_2$  nanoparticles were prepared according to our previous method [27]. GOD was immobilized on the nanoparticles using the similar chemical crosslinking method [27] to form the magnetic immobilized GOD ( $\text{Fe}_3\text{O}_4@/\text{SiO}_2(\text{F})@/\text{meso-SiO}_2@/\text{GOD}$ ). The preparation procedure of PMIGC was depicted as follows. 150 mg NIPAAm, 18 mg AAm, 7 mg BIS were dissolved in 3 mL of immobilized enzyme solution containing 90 mg nanoparticles and 12 mg GOD. The mixture was stirred at room temperature for 30 min under the protection of nitrogen. 30  $\mu\text{L}$  of TEMED and 70  $\mu\text{L}$  of APS (5 wt%) were added in it. The mixture was kept at  $-20^\circ\text{C}$  for 12 h and PMIGC was formed. The product was immersed in distilled water for 48 h and the water was refreshed every several hours in order to allow the unreacted chemicals to

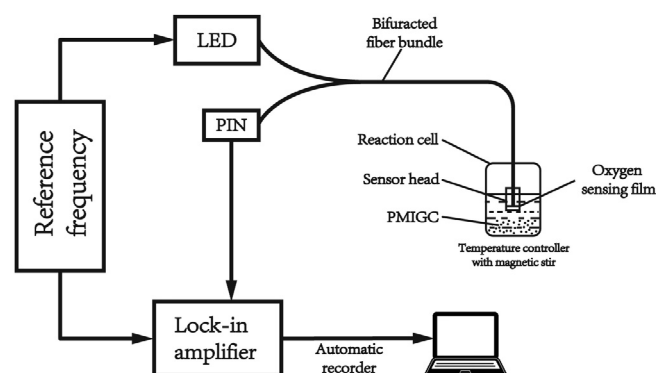


Fig. 1. Schematic diagram of the detecting system.

leach out. PMIGC was stored in distilled water at  $4^\circ\text{C}$ . The LCST of PMIGC was determined according to the reported method [29].

### 2.3. Preparation and principle of temperature controlling fiber optic glucose sensor

The detecting system is shown in Fig. 1. It consists of a lock-in amplifier, a light source of light emitting diode (LED) with an excitation wavelength of 416 nm, a sensor head with an oxygen sensing membrane, a temperature controller, and a computer for data processing.

This sensor was based on the fluorescence quenching and oxygen consumption. GOD catalyzed the oxidation of glucose and the oxygen in the solution would be consumed. By detecting the fluorescence of  $\text{Ru}(\text{bpy})_3\text{Cl}_2$  quenched by oxygen the oxygen concentration change was detected. Since a lock-in amplifier is used, the quenching could be described as

$$\frac{\tan \phi_0}{\tan \phi} = 1 + K_{sv}[Q] \quad (1)$$

Where  $\phi_0$  and  $\phi$  are the phase delay change of the sensor in the absence and presence of the oxygen, respectively, and  $K_{sv}$  is the Stern-Volmer constant.  $[Q]$  is the oxygen concentration. The quantification of glucose is achieved by detecting the data of phase delay change  $\phi$ .

### 2.4. Measurements

The detection of glucose concentration was performed with the setup shown schematically in Fig. 1. The sensor head was placed into a tiny reaction cell containing glucose buffer solution and PMIGC. In order to eliminate the interference of oxygen from the open air, an entire airtight reaction cell was introduced. A temperature controller was used to control the temperature of the reaction cell. The fluorescence signal was collected by positive intrinsic negative (PIN) and guided to the lock-in amplifier through the output bundle, and then transferred to phase-delay which was collected by the computer. After a simple washing of the sensor head and PMIGC with buffer solution, the following measurement could be performed. The magnetic core of immobilized GOD could make the isolation of PMIGC from the reaction solution and buffer faster and easier. All the measurements were performed in triplicate.

### 2.5. Characterizations

The morphology of P(NIPAAm-co-AAm) and PMIGC was observed using a field emission scanning electron microscope (FESEM) (JSM-5610LV, JEOLLtd., Japan) operated at 10 kV. Before FESEM test, the swollen hydrogel samples were quickly frozen in liquid nitrogen and then lyophilized in a freeze drier (ALPHA

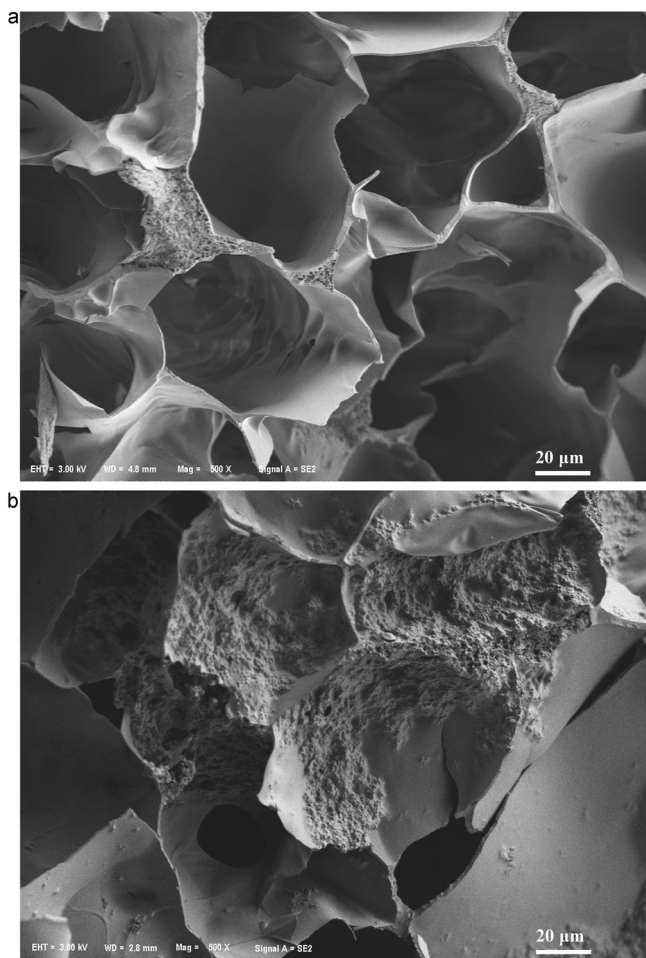


Fig. 2. SEM of P(NIPAAm-co-AAm) (A) and PMIGC (B).

1-4/2-4 LSC, Germany) under a vacuum at  $-89^{\circ}\text{C}$  for 2 days. IR spectra were recorded on a Thermo Nicolet Nexus Fourier Transform Infrared (FT-IR) spectrometer with the standard KBr pellet method. A lock-in amplifier (SR830, Stanford Research System, U. S. A.) was used for measuring the phase delay of the sensor head.

### 3. Results and discussion

#### 3.1. Characterization of PMIGC

The SEM image of the cross-section of the freeze-dried P(NIPAAm-co-AAm) is shown in Fig. 2 (A). The cross-section of the sample exhibits porous network structure. After the complex of hydrogel with the immobilized GOD, the immobilized GOD located in the holes of hydrogel, as shown in Fig. 2 (B). From Fig. 2, it can be seen that the pore diameters of P(NIPAAm-co-AAm) and PMIGC are around 60 μm.

Fig. 3 shows the IR spectra of P(NIPAAm-co-AAm), immobilized GOD and PMIGC. In the IR spectrum of PMIGC (Fig. 3(c)), the absorptions at  $1658\text{ cm}^{-1}$  and  $1548\text{ cm}^{-1}$  are characteristic peaks of amide I and amide II, and the bands of symmetric C–H bending from the  $-\text{CH}(\text{CH}_3)_2$  at  $1389$  and  $1368\text{ cm}^{-1}$  were also observed, indicating the formation of P(NIPAAm-co-AAm) [30,31]. The two bands of amide I and amide II for GOD were also at around  $1658\text{ cm}^{-1}$  and  $1548\text{ cm}^{-1}$  [32]. The absorption at  $587\text{ cm}^{-1}$  was assigned to Fe-O stretching vibration [33]. The absorption at  $1088\text{ cm}^{-1}$  was due to asymmetric stretching of the Si-O-Si chain [32]. Since the absorptions besides those of hydrogel and immobilized GOD could not be

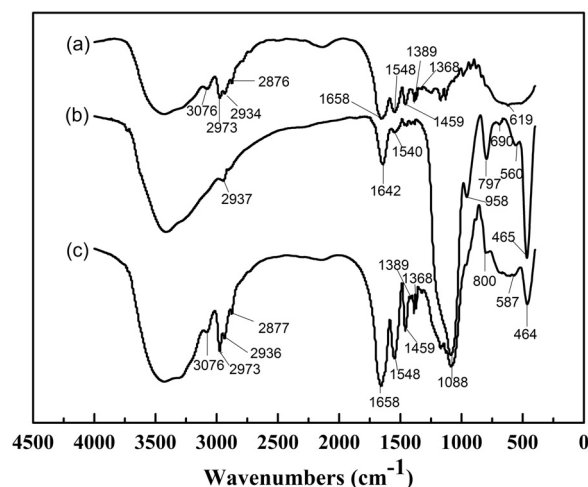


Fig. 3. IR spectra of P(NIPAAm-co-AAm) (a), immobilized GOD (b) and PMIGC (c).

observed, it can be concluded that the complex between hydrogel and magnetic complex nanoparticles was physical complex instead of chemical bonding.

#### 3.2. Oxidation of GOD catalyzed controllably by PMIGC and influence factors to the phase delay of the sensor head

According to the reported method [29], the LCST of PMIGC was determined to be  $36^{\circ}\text{C}$ . Hydrogel will swell when the temperature is lower than LCST and shrink when the temperature is higher than LCST.  $\phi$  was defined as the difference between the phase delay of the sensor head with glucose concentration of 500 mg/dL and with no glucose in the solution. As shown in Fig. 4 (A), at  $38^{\circ}\text{C}$  (above LCST), no catalysis effect for glucose oxidation was observed for PMIGC because the hydrogel shrank and separated GOD from glucose. However, at  $25^{\circ}\text{C}$  (below LCST), PMIGC had catalysis effect due to the fact that hydrogel swelled and GOD could come into contact with glucose. Therefore, by changing the reaction temperature the enzyme performance can be controlled and PMIGC had an “on-off” effect for the catalysis to GOD oxidation. The switch time for this “on-off” process was less than 1 min, which was satisfactory for the sensor.

To investigate the influence of pH, temperature and GOD amount on the sensor properties,  $\phi$  was defined as the difference between the phase delay of the sensor head with glucose concentration of 300 mg/dL and with no glucose in the solution.

It is well known that the pH of aqueous working media will significantly influence the response of a biosensors. For this fiber optic glucose biosensor, the pH effect was studied over the range of 5.0–9.0. This was performed by continuously monitoring  $\phi$  of the biosensor on exposure to 300 mg/dL glucose solution with different pH and the results were shown in Fig. 4 (B). It can be seen that  $\phi$  increased with the increase of solution pH and reached maximal value at pH 6.5. When the pH was higher than 6.5,  $\phi$  decreased with the increase of pH. The sensor performance was mainly influenced by the enzyme properties. The optimal pH for free GOD was found to be 6.0 [34]. After GOD was immobilized on  $\text{Fe}_3\text{O}_4@\text{SiO}_2(\text{F})@\text{meso-SiO}_2$  nanoparticles and then formed PMIGC, the microenvironment of immobilized enzyme and the bulk solution usually have unequal partitioning of  $\text{H}^+$  and  $\text{OH}^-$  concentration due to electrostatic interaction of enzyme with the carrier, which often leads to the shift of optimal pH [35]. Therefore, the optimal pH for the sensor was observed at 6.5. In our later experiments pH 6.5 was selected as the optimal pH.

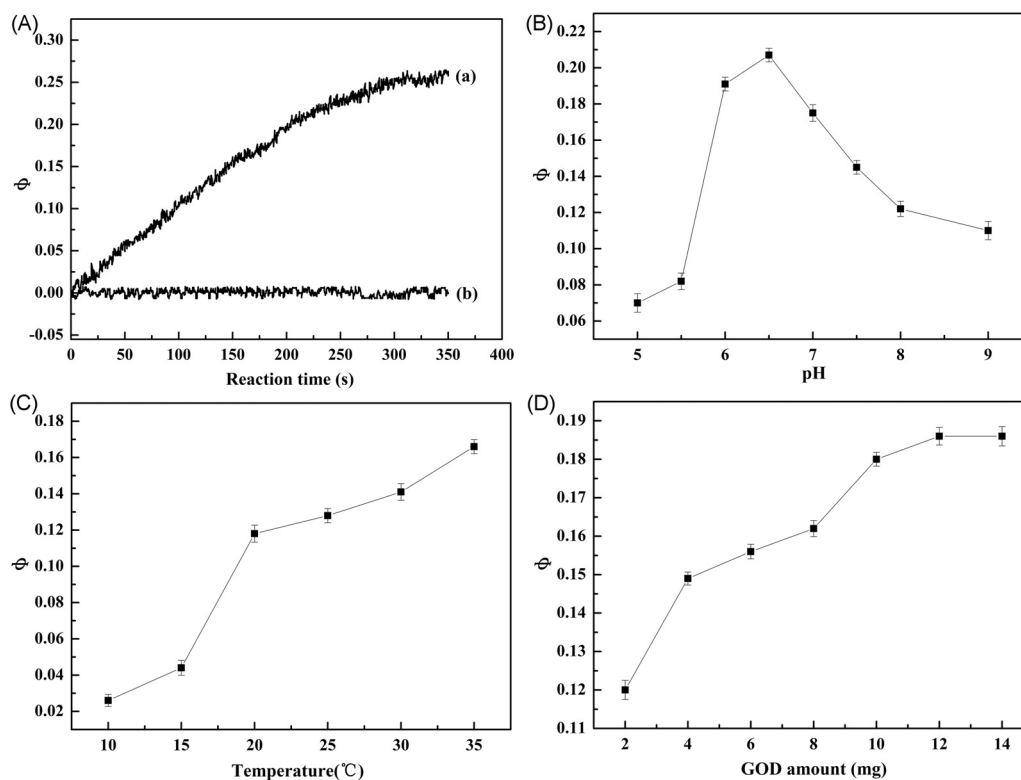


**Fig. 4.** (A) Response curves of PMIGC toward glucose of 500 mg/dL at 25 °C (a) and 38 °C (b); (B) pH effect on the response of the sensor. Glucose concentration: 300 mg/dL, room temperature, GOD amount: 12 mg (in 90 mg carrier); (C) Temperature effect on the response of sensor. Glucose concentration: 300 mg/dL, pH = 6.5, GOD amount: 12 mg (in 90 mg carrier); (D) Effect of GOD amount on the response of sensor. Glucose concentration: 300 mg/dL, pH = 6.5, room temperature. The error bars represent the standard error derived from three repeated measurements.

The effect of temperature on this sensor was studied over the range of 10 °C–35 °C because higher temperature will cause the shrink of PMIGC. As shown in Fig. 4(C), in the range of 10 °C–20 °C,  $\phi$  increased sharply with the increase of temperature and in the range of 20 °C–35 °C,  $\phi$  increased slowly with the increase of temperature and 35 °C was the optimal temperature. Free GOD was strongly dependent on temperature. It has the optimal temperature of 30 °C and higher temperature would cause a sharp decrease of enzyme activity [34]. After the immobilization on carrier, GOD would exhibit excellent activity at higher temperature [34] because the immobilization of GOD can restrict unfolding and nonspecific aggregation of the enzyme molecule, and then the thermal stability of enzyme at elevated temperatures can be improved by immobilization [36]. However, the LCST of PMIGC was 36 °C and the hydrogel would shrink at the temperature higher than 36 °C. PMIGC would not perform the catalysis to GOD oxidation when the temperature was 36 °C or higher. Therefore, the optimal temperature for this sensor is 35 °C. For the convenience of practical detection, room temperature would be selected as the working temperature since the sensor response was satisfactory at room temperature.

The effect of GOD amount was studied (GOD was immobilized on 7.5 times carrier). As shown in Fig. 4(D), the phase delay change  $\phi$  of the sensor head increased with the increase of GOD amount from 2 mg to 12 mg and decreased slightly when GOD amount was higher than 12 mg. The increase of GOD amount was in favor of oxidation of glucose. However, after the saturation of enzyme, further increase of GOD amount will cause special steric hindrance to enzyme activity. In addition, excessive GOD might form enzymatic aggregation in PMIGC, which will block the active sites of enzyme. Therefore, the optimal GOD amount for this sensor was 12 mg which was used in our later experiments.

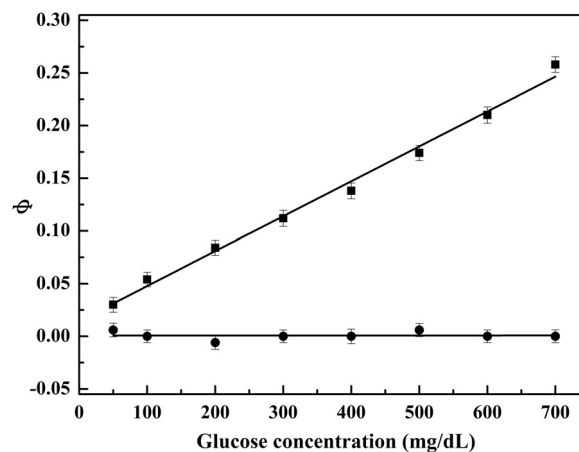


**Fig. 5.** Response curves at various concentrations of glucose at 25 °C (■) and 38 °C (●). GOD amount: 12 mg (in 90 mg carrier), pH = 6.5. The error bars represent the standard error derived from three repeated measurements.

### 3.3. Sensor properties

#### 3.3.1. Typical response curve

The biosensor could detect glucose controllably at different temperatures. At 38 °C (above LCST), PMIGC shrank and exhibited no catalysis effect for glucose oxidation and  $\phi$  was 0 for different concentrations of glucose (Fig. 5). However, at 25 °C (below LCST), the PMIGC swelled and exhibited notable catalysis effect on glucose oxidation and a good linear relationship between the phase delay change  $\phi$  of the sensor head and the glucose concentration in the range of 50–700 mg/dL (2.78–38.89 mmol/L) was observed (Fig. 5). The linear graph is defined by the equation



**Table 1**  
Interference test of the fiber optic glucose sensor on exposure to various interferents.

Interference term	[S](mg/dL)	Interference rate (%) <sup>a</sup> (C−C <sub>0</sub> )/C <sub>0</sub> × 100%
Fructose	1800	−2.78
Vitamin C	25.54	2.27
Urea	2514.9	1.00
Glycine	75.3	2.27
Cysteine	60.58	1.33
Na <sup>+</sup>	4149.24	1.92
K <sup>+</sup>	1118.25	−3.70
Ca <sup>2+</sup>	1387.25	0.91
Mg <sup>2+</sup>	541.7	−1.85
HPO <sub>4</sub> <sup>2−</sup>	1141.1	−3.7
SO <sub>4</sub> <sup>2−</sup>	106.53	2.1
HCO <sub>3</sub> <sup>−</sup>	1361	1.67
Cl <sup>−</sup>	3010	1.28

<sup>a</sup> C is the detected concentration and C<sub>0</sub> is actual concentration.

**Table 2**  
Determination of glucose in practical samples using the proposed sensor.

Sample	Glucose added (mg/dL)	Glucose found (mg/dL)	Recovery Rate(%)
1 (ABF)	100	96.27 ± 2.46	96.27
2 (ABF)	300	293.34 ± 2.13	97.78
3 (ABF)	500	516.4 ± 1.73	103.28
4 (HS)	100	97.22 ± 2.09	97.22
5 (HS)	300	294.63 ± 1.97	98.21

of  $y = 0.01463 + 0.0003313x$ ,  $R^2 = 0.9914$ . The response time was taken as 200 s and the detection limit was 8.33 mg/dL (S/N = 3). The glucose concentration for healthy people is in the range of 70.1–109.7 mg/dL and for diabetic patients is several times higher, therefore, this sensor has the potential for practical application.

### 3.3.2. Repeatability

To investigate the repeatability of the glucose biosensor, the sensor head was alternately exposed three times to the solution with the glucose concentration of 300 mg/dL and PBS solution with no glucose, and the phase delay changes were recorded. It was shown in Fig. 6 that there was no big difference between the three repeated detections ( $n = 3$ , RSD = 2.33%), indicating that the biosensor exhibited a satisfactory repeatability.

### 3.3.3. Lifetime

To study the lifetime of the sensor, the response value of the oxygen sensing film in contact with 200 mg/dL glucose solution was recorded after keeping the film in water for 7 days and the change of phase delay of the sensor under optimal conditions only decreases by 8.6%. One reason for the loss of sensitivity might be the indicator leaking from the film. The immobilized GOD maintains 86% of its initial activity after being stored for 1 month at 4 °C, indicating a good stability for the immobilized GOD.

### 3.3.4. Selectivity

Selectivity is another important characteristic for biosensor. This was investigated by selecting 100 mg/dL as the actual concen-

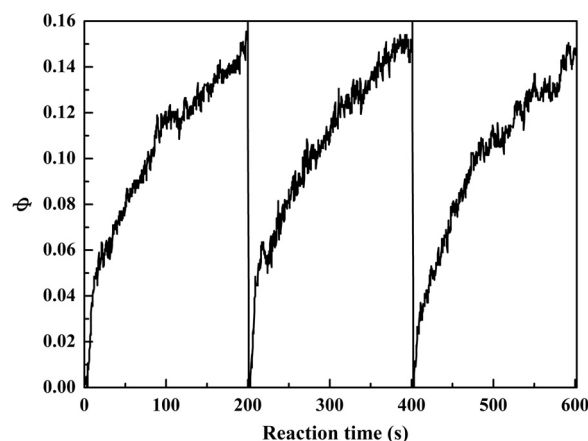


**Fig. 6.** Repeatability of the sensor. Glucose concentration: 300 mg/dL, pH = 6.5, room temperature, GOD amount: 12 mg (in 90 mg carrier).

tration of glucose and using the interference rate in the presence of potential interferents as sensor selectivity indicators. The results are shown in Table 1. It could be concluded that none of the interferents caused significant interference to the response of the sensor, showing a good selectivity of this sensor.

### 3.3.5. Real sample detection

The recovery test was performed using artificial body fluid (ABF) and human serum (HS) as the practical samples. The test was carried out with three different added glucose concentrations in ABF and two different added glucose concentrations in HS. The original glucose concentrations in ABF and HS were determined to be 0 and 83 mg/dL, respectively. The found glucose concentrations were obtained by subtracting the original glucose concentrations from the total glucose concentrations (The total glucose concentrations were determined after the addition of glucose into the ABF and HS samples) All the measurements were performed in triplicate and the results are shown in Table 2. It can be seen that the practical application of this sensor is satisfactory.

We compared our sensor with other reported methods for glucose determination. The results shown in Table 3 indicate that our sensor has good selectivity, repeatability and recovery rate, and the detection range is also satisfactory.

## 4. Conclusion

PMIGC was prepared and the controllable catalysis for the oxidation of glucose was realized by using it. Based on PMIGC, a fiber optic glucose biosensor was fabricated to perform the controllable detection of glucose by changing temperature. The optimal detection conditions for this biosensor were obtained. At 38 °C, PMIGC could not catalyze the oxidation of glucose and the biosensor was unable to perform the determination of glucose. At 25 °C, a good linear relationship between  $\phi$  and the glucose concentration in the range of 50–700 mg/dL was observed. This biosensor has the characteristics of good repeatability, selectivity and can be used for

**Table 3**  
Comparison of the proposed sensor with other glucose detection methods.

Method	Detection range (mmol/L)	Selectivity	Repeatability (RSD(%))	Recovery rate (%)	Ref.
HPLC	0.0056–0.56	–	2.56	101–103	[37]
Quantum Dots	0.005–0.4	Good	3.1	95.5–108.9	[38]
Electrochemical	$1.0 \times 10^{-5}$ –80	Good	4.60	90.1–104.8	[39]
Chemiluminescence	$8.5 \times 10^{-4}$ –0.1	Good	2.9	93.8–110.1	[40]
Colorimetry	0.3–1.0	–	3.68	97.68–103.27	[41]
Proposed sensor	0.46–38.89	Good	2.33	96.27–103.28	This work

the determination of glucose concentration in practical samples, showing a promising prospect for practical application.

Furthermore, by using PMIGC and immobilized COD and controlling the detection temperature, it will be possible to perform simultaneous determination of glucose and cholesterol. This work is currently undertaking in our laboratory.

### Acknowledgements

This study was financially supported by National Natural Science Foundation of China (No: 61377092, 61575150).

### References

- [1] S. Wild, G. Roglic, A. Green, R. Sicree, H. King, Global prevalence of diabetes: estimates for the year 2000 and projections for 2030, *Diabetes Care* 27 (2004) 1047–1053.
- [2] P. Lu, J. Yu, Y. Lei, S. Lu, C. Wang, D. Liu, Q. Guo, Synthesis and characterization of nickel oxide hollow spheres-reduced graphene oxide-nafion composite and its biosensing for glucose, *Sens. Actuators B* 208 (2015) 90–98.
- [3] T. Sato, K. Katayama, T. Arai, T. Sako, H. Tazaki, Simultaneous determination of serum mannose and glucose concentrations in dog serum using high performance liquid chromatography, *Res. Vet. Sci.* 84 (2008) 26–29.
- [4] S. Song, L. Sun, L. Yuan, T. Sun, Y. Zhao, W. Zuo, Y. Cong, X. Li, J. Wang, Method to determine enantiomeric excess of glucose by nonchiral high-performance liquid chromatography using circular dichroism detection, *J. Chromatogr. A* 1179 (2008) 125–130.
- [5] Q. Liu, L. Hui, Q. Zhao, R. Zhu, Y. Yang, Q. Jia, B. Bing, L. Zhuo, Glucose-sensitive colorimetric sensor based on peroxidase mimics activity of porphyrin-Fe<sub>3</sub>O<sub>4</sub> nanocomposites, *Mater. Sci. Eng. C* 41 (2014) 142–151.
- [6] W.I. Kanchana, T. Sakai, N. Teshima, S. Katoh, K. Grudpan, Successive determination of urinary protein and glucose using spectrophotometric sequential injection method, *Anal. Chim. Acta* 604 (2008) 139–146.
- [7] M.J. Chaichi, S.O. Alijanpour, Chitosan-induced Au/Ag nanoalloy dispersed in IL and application in fabricating an ultrasensitive glucose biosensor based on luminol-H<sub>2</sub>O<sub>2</sub>-Cu<sup>2+</sup>/IL chemiluminescence system, *J. Photochem. B* 140 (2014) 41–48.
- [8] X. Liu, W. Niu, H. Li, H. Shuang, L. Hu, G. Xu, Glucose biosensor based on gold nanoparticle-catalyzed luminol electrochemiluminescence on a three-dimensional sol-gel network, *Electrochem. Commun.* 10 (2008) 1250–1253.
- [9] B. Qiu, M. Miao, L. She, X. Jiang, Z.Y. Lin, G.N. Chen, An ultrasensitive biosensor for glucose based on solid-state electrochemiluminescence on GOx/CdS/GCE electrode, *Anal. Methods* 5 (2013) 1941–1945.
- [10] T. Alizadeh, S. Mirzagholidpur, An outstandingly sensitive enzyme-free glucose sensor prepared by co-deposition of nano-sized cupric oxide and multi-walled carbon nanotubes on glassy carbon electrode, *Biochem. Eng. J.* 97 (2015) 81–91.
- [11] P. Lu, Q.B. Liu, Y.Z. Xiong, Q. Wang, Y.T. Lei, S.J. Lu, L.W. Lu, L. Yao, Nanosheets-assembled hierarchical microstructured Ni(OH)<sub>2</sub> hollow spheres for highly sensitive enzyme-free glucose sensors, *Electrochim. Acta* 168 (2015) 148–156.
- [12] A.Y. Khan, S.B. Noronha, R. Bandyopadhyaya, Glucose oxidase enzyme immobilized porous silica for improved performance of a glucose biosensor, *Biochem. Eng. J.* 91 (2014) 78–85.
- [13] Z. Li, X. Miao, A. Zhu, L. Ling, Hybridization chain reaction and gold nanoparticles dual signal amplification for sensitive glucose detection, *Biochem. Eng. J.* 103 (2015) 205–210.
- [14] C.P. Huang, S.W. Liu, T.M. Chen, Y.K. Li, A new approach for quantitative determination of glucose by using CdSe/ZnS quantum dots, *Sens. Actuators B* 130 (2008) 338–342.
- [15] L.Y. Ding, B.Y. Zhang, C. Xu, J. Huang, Z.L. Xia, Fluorescent glucose sensing using CdTe/CdS quantum dots-glucose oxidase complex, *Anal. Methods* 8 (2016) 2967–2970.
- [16] J.P. Yuan, W.W. Guo, E.K. Wang, Quantum dots-bi-enzyme hybrid system for the sensitive determination of glucose, *Biosens. Bioelectron.* 23 (2008) 1567–1571.
- [17] X.D. Wang, T.Y. Zhou, X. Chen, K.Y. Wong, X.R. Wang, An optical biosensor for the rapid determination of glucose in human serum, *Sens. Actuators B* 129 (2008) 866–873.
- [18] A.L. Hu, Y.H. Liu, H.H. Deng, G.L. Hong, A.L. Liu, X.H. Lin, X.H. Xia, W. Chen, Fluorescent hydrogen peroxide sensor based on cupric oxide nanoparticles and its application for glucose and L-lactate detection, *Biosens. Bioelectron.* 61 (2014) 374–378.
- [19] G. Chang, Y. Tatsu, T. Goto, H. Imaishi, K. Morigaki, Glucose concentration determination based on silica sol-gel encapsulated glucose oxidase optical biosensor arrays, *Talanta* 83 (2010) 61–65.
- [20] O.S. Wolfbeis, Fiber-optic chemical sensors and biosensors, *Anal. Chem.* 78 (2006) 3859–3874.
- [21] Y. Qiu, K. Park, Environment-sensitive hydrogels for drug delivery, *Adv. Drug Deliver. Rev.* 53 (2001) 321–339.
- [22] B. Wang, X.D. Xu, Z.C. Wang, S.X. Cheng, X.Z. Zhang, R.X. Zhuo, Synthesis and properties of pH and temperature sensitive P(NIPAAm-co-DMAEMA) hydrogels, *Colloids Surf. B* 64 (2008) 34–41.
- [23] G. Fundueanu, M. Constantin, P. Ascenzi, Fast-responsive porous thermoresponsive microspheres for controlled delivery of macromolecules, *Int. J. Pharm.* 379 (2009) 9–17.
- [24] N.S. Satarkar, H.J. Zach, Hydrogel nanocomposites as remote-controlled biomaterials, *Acta Biomater.* 4 (2008) 11–16.
- [25] J.T. Zhang, T.F. Keller, R. Bhat, B. Garipcan, K.D. Jandt, A novel two-level microstructured poly(N-isopropylacrylamide) hydrogel for controlled release, *Acta Biomater.* 6 (2010) 3890–3898.
- [26] X.Z. Zhang, R.X. Zhuo, Dynamic properties of temperature-sensitive poly(N-isopropylacrylamide) gel cross-linked through siloxane linkage, *Langmuir* 17 (2000) 12–16.
- [27] J. Huang, H.C. Liu, P.P. Zhang, P.F. Zhang, M.S. Li, L. Ding, Immobilization of cholesterol oxidase on magnetic fluorescent core-shell-structured nanoparticles, *Mater. Sci. Eng. C* 57 (2015) 31–37.
- [28] J. Huang, H. Fang, C. Liu, E.D. Gu, D.S. Jiang, A novel fiber optic biosensor for the determination of adrenaline based on immobilized laccase catalysis, *Anal. Lett.* 41 (2008) 1430–1442.
- [29] X.Z. Zhang, Y.Y. Yang, T.S. Chung, K.X. Ma, Preparation and characterization of fast response macroporous poly(N-isopropylacrylamide) hydrogels, *Langmuir* 17 (2001) 6094–6099.
- [30] J. Chen, J. Sun, L. Yang, Q. Zhang, H. Zhu, H. Wu, A.S. Hoffman, I. Kaetsu, Preparation and characterization of a novel IPN hydrogel membrane of poly(N-isopropylacrylamide)/carboxymethyl chitosan (PNIPAAm/CMCS), *Radiat. Phys. Chem.* 76 (2007) 1425–1429.
- [31] M. Avadanei, O. Avadanei, G. Fundueanu, Effect of comonomer ratio and ionic strength on the thermo-induced conformational changes in N-isopropylacrylamide based copolymers: an ATR-FTIR spectroscopic study, *Vib. Spectrosc.* 61 (2012) 133–143.
- [32] I. Delfino, M. Portaccio, B.D. Ventura, D.G. Mita, M. Lepore, Enzyme distribution and secondary structure of sol-gel immobilized glucose oxidase by micro-attenuated total reflection FT-IR spectroscopy, *Mater. Sci. Eng. C* 33 (2013) 304–310.
- [33] C.L. Lin, C.F. Lee, W.Y. Chiu, Preparation and properties of poly(acrylic acid) oligomer stabilized superparamagnetic ferrofluid, *J. Colloid Interface Sci.* 291 (2005) 411–420.
- [34] J. Huang, H. Wang, D. Li, W. Zhao, L. Ding, Y. Han, A new immobilized glucose oxidase using SiO<sub>2</sub> nanoparticles as carrier, *Mater. Sci. Eng. C* 31 (2011) 1374–1378.
- [35] A. Martino, P.G. Pifferi, G. Spagna, Immobilization of β-glucosidase from a commercial preparation. Part 2. Optimization of the immobilization process on chitosan, *Process Biochem.* 31 (1996) 287–293.
- [36] L. Zhou, Y. Jiang, J. Gao, X. Zhao, L. Ma, Q. Zhou, Oriented immobilization of glucose oxidase on graphene oxide, *Biochem. Eng. J.* 69 (2012) 28–31.
- [37] M. Grembecka, A. Lebidzińska, P. Szefer, Simultaneous separation and determination of erythritol xylitol, sorbitol, mannitol, maltitol, fructose, glucose, sucrose and maltose in food products by high performance liquid chromatography coupled to charged aerosol detector, *Microchem. J.* 117 (2014) 77–82.
- [38] H. Zhai, T. Feng, L. Dong, L. Wang, X. Wang, H. Liu, Y. Liu, L. Chen, M. Xie, Development of dual-emission ratiometric probe-based on fluorescent silica nanoparticle and CdTe quantum dots for determination of glucose in beverages and human body fluids, *Food Chem.* 204 (2016) 444–452.
- [39] Y. Luo, F.Y. Kong, C. Li, J.J. Shi, W.X. Lv, W. Wang, One-pot preparation of reduced graphene oxide-carbon nanotube decorated with Au nanoparticles based on protein for non-enzymatic electrochemical sensing of glucose, *Sens. Actuators B* 234 (2016) 625–632.
- [40] M.J. Chaichi, M. Ehsani, A novel glucose sensor based on immobilization of glucose oxidase on the chitosan-coated Fe<sub>3</sub>O<sub>4</sub> nanoparticles and the luminol-H<sub>2</sub>O<sub>2</sub>-gold nanoparticle chemiluminescence detection system, *Sens. Actuators B* 223 (2015) 713–722.
- [41] C. Xi, C. Jin, F. Wang, X. Xia, L. Ming, X. Ji, Z. He, Determination of glucose and uric acid with bi-enzyme colorimetry on microfluidic paper-based analysis devices, *Biosens. Bioelectron.* 35 (2012) 363–368.